Non-binary turbo-coded physical-layer network coding on impulsive noise channels

Yuanyi Zhao✉, Martin Johnston, Charalampos Tsimenidis and Li Chen

Non-binary turbo codes promise excellent performance for a wide range of applications and environments, but research in this area is sparse. The performance of a non-binary turbo code defined in GF (4) on a two-way wireless relay channel (TWRC) employing physical-layer network coding, which is affected by impulsive noise is investigated. Simulation results for binary and non-binary turbo codes are presented and validated with an error floor analysis at the relay of the TWRC and it is observed that non-binary turbo codes significantly outperform binary turbo codes at low signal-to-noise ratios.

Introduction: Physical-layer network coding (PNC) is a popular technique applied to two-way wireless relay channels (TWRC) [1] that exploits interference at a relay node to boost throughput. Combining PNC with error correction offers further improvements in performance, but there is only a small body of work on turbo codes on the TWRC. This includes Hausl and Philippe [2] who proposed a distributed turbo coding scheme for a multiple access relay channel and Fang and Burr [3] who studied the performance degradation of binary turbo codes on a TWRC. Interestingly, there appears to be no work in the literature studying non-binary turbo codes with PNC. In [4], Berrou and Jezequel introduced non-binary convolutional codes for turbo coding and showed that quaternary codes can be advantageous, both in terms of performance and complexity. Hence, in this Letter we investigate the performance of non-binary turbo codes over GF(4) combined with PNC, where encoding and decoding take place at the relay and source/destination nodes in both time slots. We also consider the effect of additive impulsive noise on the performance of non-binary turbo codes at the relay. This has been investigated in [5] for binary turbo codes, where the authors analysed the performance of binary turbo codes combined with PNC on additive impulsive noise channels. Following on from this work, we now investigate the effect of impulsive noise on the iterative non-binary turbo decoder employed at the relay of a TWRC and compare it with a binary turbo decoder under the same conditions.

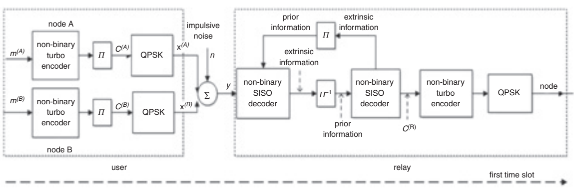

Fig. 1 *System model showing turbo encoder and iterative decoding process of PNC system*

To evaluate the performance of a turbo decoder effected by impulsive noise, we need to know the probability density function (pdf) of the noise. To achieve this, the Gaussian mixture model (GMM) has been selected [6] with a pdf, $p_{\text{GMM}}(x)$, that is defined as: $p_{\text{GMM}}(x) = (1-\alpha)p_{\text{G}}(x) + \alpha p_{\text{I}}(x)$, where $0 \le \alpha \le 1$ is the mixture constant, with larger values of α denoting more impulsiveness. The terms $p_{\text{G}}(x)$ and $p_{\text{I}}(x)$ are two Gaussian pdfs, where $p_{\text{I}}(x)$ has a much larger variance than $p_{\text{G}}(x)$, and $p_{\text{GMM}}(x)$ is the resulting impulse noise pdf.

System model: The system model of the conventional TWRC employing turbo codes combined with PNC is shown in Fig. 1. Two source nodes, A and B, have no direct link to each other and must transmit their messages through the relay R. Let $m_k^{(A)}, m_k^{(B)} \in \{0, 1, \beta, \beta^2\}$ denote the kth message symbol defined in GF(4) sent from node A and node B, respectively, where β is a primitive element in GF(4). The messages are encoded to obtain the coded symbol $c_k^{(A)}, c_k^{(B)} \in \{0, 1, \beta, \beta^2\}$. The received information sequence at the relay can be expressed as: $y_k = x_k^{(A)} + x_k^{(B)} + \eta_k$, where $x_k^{(A)}$ and $x_k^{(B)}$ are quadrature phase shift keying (QPSK) symbols from nodes A and B, respectively, and η_k is the noise added at the relay. The relay must then determine the log-likelihood ratios (LLR) of y_k given that $x_k^{(R)} = x_k^{(A)} + x_k^{(B)}$ was transmitted. These LLRs are decoded at the relay to obtain a message that represents the finite field sum of $m_k^{(A)}$ and $m_k^{(B)}$. The decoded message is then re-encoded to obtain $c_k^{(R)}$, which is mapped to the QPSK constellation and broadcast back to nodes A and B. At nodes A and B, the received signal is decoded to obtain the message symbol $m_k^{(R)}$, where node A can obtain $m_k^{(B)}$ by performing the bitwise addition of $m_k^{(R)}$ with its known binary message symbols $m_k^{(A)}$. A similar operation is performed at node B to obtain $m_k^{(A)}$.

Gaussian mixture receiver design: When QPSK modulation is employed at the source nodes, the received symbol at the relay can have one of nine complex values resulting from all possible additions of the two signals $x_k^{(A)}$ and $x_k^{(B)}$. Each of the nine constellation points maps to one of the finite field elements $z \in \text{GF}(q)$. Let X be the set of the nine points, then $X_z \subset X$ is the subset of points corresponding to the element z. Assuming the QPSK modulation scheme has unit energy, then the subsets are: $X_0 = \{0\}$, $X_1 = \{-2j, 2j\}$, $X_\beta = \{-2, 2\}$ and $X_{\beta^2} = \{2+2j, 2-2j, -2+2j, -2-2j\}$. The conditional LLRs of the received symbols are defined as

$$L^{(z)}(c_k^{(R)}|y_k) = \ln\left(\frac{P(c_k^{(R)} = z|y_k)}{P(c_k^{(R)} = 0|y_k)}\right) = \ln\left(\frac{\sum_{x_k^{(R)} \in X_z} P(x_k^{(R)}|y_k)}{\sum_{x_k^{(R)} \in X_0} P(x_k^{(R)}|y_k)}\right) \quad (1)$$

where $L^{(z)}(c_k^{(R)}|y_k)$ is the LLR denoting the reliability of the coded symbol being z given that we receive y_k. According to Baye's rule, $L^{(z)}(c_k^{(R)}|y_k)$ at the relay can be written as

$$\begin{aligned} L^{(z)}(c_k^{(R)}|y_k) &= \ln\left(\frac{P(c_k^{(R)} = z)P(y_k|c_k^{(R)} = z)}{P(c_k^{(R)} = 0)P(y_k|c_k^{(R)} = 0)}\right) \\ &= \ln\left(\frac{P(y_k|c_k^{(R)} = z)}{P(y_k|c_k^{(R)} = 0)}\right) + \ln\left(\frac{P(c_k^{(R)} = z)}{P(c_k^{(R)} = 0)}\right) \\ &= L^{(z)}(y_k|c_k^{(R)}) + L^{(z)}(c_k^{(R)}) \end{aligned} \quad (2)$$

where the term $L^{(z)}(c_k^{(R)})$ is the a priori LLR and for the GMM receiver

$$L^{(z)}(y_k|c_k^{(R)}) = \ln\left(\frac{\sum_{x_R \in X_z} \alpha\, e^{-(|y_k - x_R|^2/2\sigma_{\text{I}}^2)} + (1-\alpha)\, e^{-(|y_k - x_R|^2/2\sigma_{\text{G}}^2)}}{\sum_{x_R \in X_0} \alpha\, e^{-(|y_k - x_R|^2/2\sigma_{\text{I}}^2)} + (1-\alpha)\, e^{-(|y_k - x_R|^2/2\sigma_{\text{G}}^2)}}\right) \quad (3)$$

where σ_{G}^2 and σ_{I}^2 are the noise variance of Gaussian noise and impulsive noise, respectively.

In this Letter, the non-binary turbo decoder employs the log-MAP algorithm for each component decoder, where the forward and backward recursion metrics, A and B, and branch metrics, γ, are defined as

$$A_{k+1}(s) = \max_{\hat{s}}\{A_k(\hat{s}) + \gamma_k(\hat{s}, s)\} \quad (4)$$

$$B_k(\hat{s}) = \max_{s}\{B_{k+1}(s) + \gamma_k(\hat{s}, s)\} \quad (5)$$

$$\gamma_k(\hat{s}, s) = L^{(z)}(c_k^{(R)}) + \max_{x_R \in X_z}\left\{-\frac{|y_k - x_R|^2}{2\sigma_{\text{GMM}}^2}\right\} \quad (6)$$

where $\hat{s}$ and s are the current state and the next state at time k and $k+1$, respectively. The calculation of the decoder output LLRs are

$$\begin{aligned} L^{(z)}(c_k^{(R)}|y_k) = &\max_{\hat{s}-s \in S_z}[A_{k-1}(\hat{s}) + \gamma_k(\hat{s}, s) + B_k(s)] \\ &- \max_{\hat{s}-s \in S_0}[A_{k-1}(\hat{s}) + \gamma_k(\hat{s}, s) + B_k(s)] \end{aligned} \quad (7)$$

where S_z is the set of all state transitions corresponding to $c_k^{(R)} \neq 0$ and S_0 is the set of all state transitions corresponding to $c_k^{(R)} = 0$.

Results and discussion: The non-binary turbo code in this Letter is defined in GF(4) and has a code rate of 1/3. It is formed from the rate $1/2(\beta\beta^2/1)$ recursive systematic non-binary convolutional code, which has a constraint length of 2, two feed-forward coefficients β and β^2 with feedback coefficient of 1 that has an optimal free distance of 10, as shown in Fig. 2 [5]. We compare this code with a rate 1/3 binary turbo code, formed from the $(1, 7/5)_8$ recursive systematic convolutional code with a constraint length of 3 and a free distance of 10.

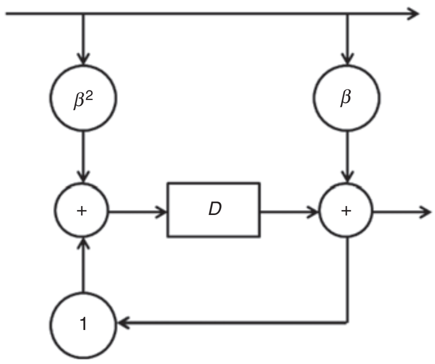

Fig. 2 *Rate (1/2) ($1\beta\beta^2/1$) four-ary convolutional encoder*

When there is no impulsive noise ($\alpha = 0$), Fig. 3 shows that the performance of both the binary and non-binary turbo code at the relay converge at an signal-to-noise ratio (SNR) of 4 dB, but the non-binary turbo code has better performance at low SNR. We observe this behaviour for the performance of both codes on impulsive noise channels. The performance of coded PNC is seriously affected by additive impulsive noise resulting in error floors, as shown in Fig. 3. From the figure it can be seen that the non-binary turbo code has an advantage at low SNRs due to its symbol-error correction instead of bit-error correction. When $\alpha = 0.01$, the non-binary turbo code has an advantage of 2 dB at a bit-error rate (BER) of 10^{-5}; for $\alpha = 0.1$, the non-binary turbo code has an even larger coding gain of 2.5 dB over the binary turbo code at a BER of 10^{-4} and then both BERs level off at an SNR of 9 dB. Furthermore, the waterfall region of the BER curve for non-binary turbo code starts at a lower SNR for all impulsive noise mixtures, e.g. when $\alpha = 0.1$, the waterfall region of the binary turbo code starts at 4 dB, which is 2 dB greater than the non-binary turbo code.

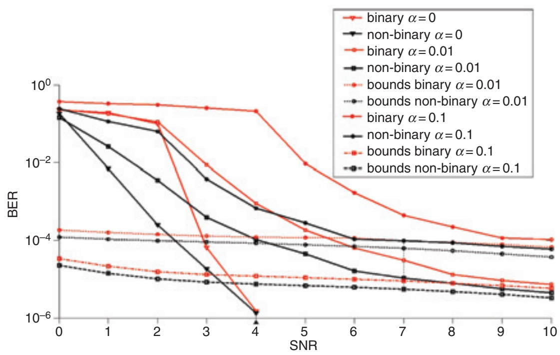

Fig. 3 *BER comparison of rate (1/3) $\beta\beta^2/1$ non-binary turbo code and rate (1/3) $(1, 7/5)_8$ binary turbo code with impulsive noise added at relay and corresponding theoretical error floors when α = 0, 0.01 and 0.1, interleaver length = 1000 symbols or 2000 bits and five decoding iterations*

To validate our simulation results, we include the theoretical lower bound on the BER performance of the non-binary turbo code at the relay to obtain its error floor. The pairwise probability at the relay when both source nodes employ QPSK modulation and PNC demapping is applied is expressed as [5]

$$P_d = \frac{3}{2} Q\left(\sqrt{2R_c d_k \frac{E_b}{N_0}}\right) \tag{8}$$

Therefore, by applying the union bound a lower bound on the bit-error probability for a turbo code at the relay is found to be

$$P_b^R \lesssim \frac{3}{2K} \sum_{w \geq 2} w n_w Q\left(\sqrt{2R_c d_{w,\min} \frac{E_b}{N_0}}\right) \tag{9}$$

where n_w denotes the number of information sequences of weight w that generate codewords of weight $d_{w,\min}$, and $d_{w,\min}$ is the minimum codeword weight among all codewords that are generated by information sequences of weight w. On the GMM impulsive noise channel, the lower bound for a turbo code at the relay is

$$P_b^{\mathrm{GMM}} \lesssim \frac{3}{2K} \sum_{w \geq 2} w n_w \left((1-\alpha)\sqrt{2R_c d_{w,\min} \frac{E_b}{N_{\mathrm{G}}}} + \alpha \sqrt{2R_c d_{w,\min} \frac{E_b}{N_{\mathrm{I}}}} \right) \tag{10}$$

where N_{G} and N_{I} are the noise power spectral densities for the Gaussian and impulsive terms in the GMM, respectively. The term $(2^{s-1}/2s - 1)$ converts the symbol-error rate to the BER and $s = \log_2(q)$. Hence, the lower bound on the BER for a non-binary turbo code at the relay can be defined as

$$P_{\mathrm{nb}}^{\mathrm{GMM}} \lesssim \frac{2^{s-1}}{2s-1} \frac{3}{2K} \sum_{w \geq 2} w n_w \left((1-\alpha)\sqrt{2R_c d_{w,\min} \frac{E_b}{N_{\mathrm{G}}}} + \alpha \sqrt{2R_c d_{w,\min} \frac{E_b}{N_{\mathrm{I}}}} \right) \tag{11}$$

We observe that, as expected, the simulated BER results in Fig. 3 converge to the theoretical lower bounds as SNR increases.

Conclusion: In this Letter, an analysis of non-binary turbo codes defined in GF(4) on a TWRC employing PNC with additive impulsive noise channels has been investigated for the first time. We have shown that the performance of turbo codes is seriously affected on the GMM noise channel when the mixture is high, but non-binary turbo codes can achieve significant improvements in performance at low SNR compared with binary turbo codes. A lower bound on the BER to determine the error floor in the presence of impulsive noise was also presented for both binary and non-binary turbo codes to validate our simulation results, where the error floor was observed to be consistently lower for non-binary turbo codes over a wide range of SNRs.

Submitted: *12 August 2016* E-first: *31 October 2016*
doi: 10.1049/el.2016.2946
One or more of the Figures in this Letter are available in colour online.

Yuanyi Zhao, Martin Johnston and Charalampos Tsimenidis (*School of Electrical and Electronic Engineering, Newcastle University, Newcastle-upon-Tyne, United Kingdom*)

✉ E-mail: y.zhao3@ncl.ac.uk

Li Chen (*School of Electronics and Information Engineering, Sun Yat-sen University, Guangzhou, People's Republic of China*)

References

1 Zhang, S., Liew, S.C., and Lam, P.P.: 'Hot topic: physical-layer network coding'. Proc. 12th Annual Int. Conf. on Mobile Computing and Networking, September 2006, pp. 358–365
2 Hausl, C., and Philippe, D.: 'Joint network channel coding for the multiple access relay channel'. IEEE Third Annual IEEE Conf. on Sensors and Ad Hoc Communications and Networks, 2006, pp. 817–822
3 Fang, D., and Burr, A.: 'Performance degradation of turbo coded physical layer network coding on the two-way relay channel'. IEEE 22nd Int. Symp. on Personal Indoor and Mobile Radio Communications (PIMRC), 2011, September 2011, pp. 1748–1752
4 Berrou, C., and Jezequel, M.: 'Non-binary convolutional codes for turbo coding', *Electron. Lett.*, 1999, **35**, (1), pp. 39–40
5 Zhao, Y., Johnston, M., Tsimenidis, C., *et al.*: 'Link-by-link coded physical layer network coding on impulsive noise channels'. IEEE Sensor Signal Processing for Defence (SSPD), September 2015, pp. 1–5
6 Middleton, D.: 'Procedures for determining the parameters of the first-order canonical models of class A and class B electromagnetic interference', *Trans. Electromagn. Compat.*, 1979, **26**, (3), pp. 190–208
7 Carrasco, R.A., and Johnston, M.: 'Non-binary error control coding for wireless communications and data storage' (John Wiley and Sons, Chichester, UK, 2008)